DOI: 10.5281/zenodo.18527045
Link: https://zenodo.org/records/18527045

NONLINEAR VIBRATIONS AND STABILITY OF VISCOELASTIC CYLINDRICAL SHELLS UNDER COMPRESSIVE LOADS

M.A. Ismanov*[a], A.I. Karimov [b].
[a] Namangan State Technical University, Namangan, Uzbekistan
[b] University of business and science, Namangan, Uzbekistan.
E-mail: ismanovm91@gmail.com.

Abstract: *In this article, the stability of a cylindrical shell is investigated in a geometric nonlinear setting. The cylindrical shell is subjected to static and dynamic influences. The shell material is orthotropic and has rheological properties that are described by the hereditary Boltzmann-Voltaire theory. The characteristic deflections equal to the shell thickness are taken as a criterion for dynamic buckling. As a result of the study, the character of measuring the deflection of the shell, taking into account the rheological properties of the material, was obtained. It was revealed that with an increase in the loading rate, the dynamic critical load increases several times in comparison with the static one.*

Keywords: *cylindrical, shell, static, dynamic, action, Boltzmann Voltaire's theory, viscosity, elasticity, ripple, nonlinearity, stability, geometry, deflection arrow, length, radius, number of half-waves, generatrix.*

1. INTRODUCTION

Thin-walled cylindrical shells are widely used in modern engineering structures such as aerospace vehicles, pipelines, pressure vessels, storage tanks, and marine constructions. These structural elements often operate under complex loading conditions that include static, dynamic, and impact-type compressive forces. Under such circumstances, the problem of stability becomes one of the most critical aspects in ensuring the reliability and safety of structures. Numerous experimental and theoretical investigations have shown that thin shells are highly sensitive to imperfections, material properties, and loading rates. In many cases, the critical loads predicted by classical linear stability theory significantly overestimate the actual buckling loads observed in practice.

To obtain more accurate predictions, it is necessary to employ geometrically nonlinear theories that take into account large deflections comparable with the shell thickness. In addition, real structural materials frequently exhibit time-dependent behavior such as creep and stress relaxation. These effects can be adequately described by viscoelastic constitutive models based on hereditary integral relations, among which the Boltzmann–Volterra theory is widely accepted. The incorporation of viscoelasticity into stability analysis allows a more realistic representation of material behavior under dynamic loading.

Another important factor influencing shell stability is the presence of initial geometric imperfections. Such imperfections inevitably arise during manufacturing, transportation, and assembly processes and can drastically reduce the load-carrying capacity of shells. Therefore, accounting for initial imperfections together with material viscoelasticity and geometric nonlinearity is essential for reliable stability assessment.

The present study is devoted to the investigation of nonlinear vibrations and dynamic stability of orthotropic viscoelastic cylindrical shells subjected to compressive loads. The governing nonlinear integro-differential equations are derived using the classical shell theory with geometric nonlinearity.

The Bubnov–Galerkin method is applied to reduce the problem to a system of ordinary differential equations, which is subsequently solved numerically using the Runge–Kutta method. The influence of loading rate, material viscosity, orthotropy, and wave numbers on the shell response and dynamic buckling behavior is analyzed in detail.

2. LITERATURE REVIEW.

Let us consider a cylindrical shell that perceives the ultimate compressive forces (Fig. 1). It is assumed that there is no wave process of stress propagation in the middle surface. Let the shell be hinged at the ends with rigid frames.

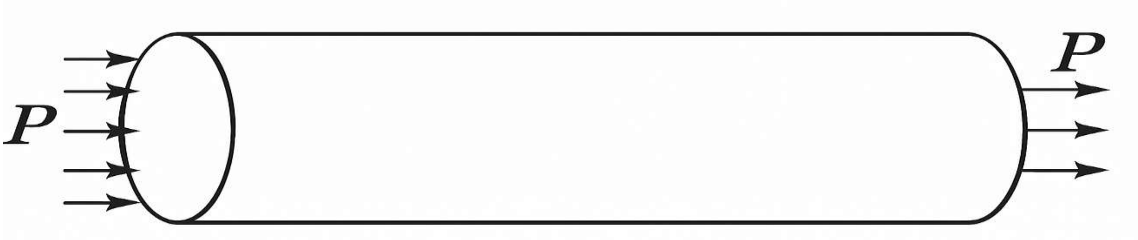

Figure 1. Cylindrical shell that can withstand extreme compressive loads.

Let us approximate the expression for the deflection of the function of spatial coordinates and time by the expression [3] corresponding to the static solutions of the first approximation, but taking into account the possible changes in the number of nodal lines in different directions.

$$w(x,y,t) = f(t)(sin\frac{mBx}{L}sin\frac{ny}{R} + \psi\, sin^2\frac{mBx}{L} + \phi_1), \quad (1)$$

parameter $f(t)$ - characterizes the deflection arrow of the shell; L - length; R - radius; m - the number of half-waves along the generatrix; n number of waves in a circle; ψ is the ratio of the "asymmetrical" component of the deflection to the symmetrical one; $f\phi_1$ defines the axisymmetric deflection associated with the "deflection" of the frames.

We consider the shell "imperfect", i.e. having some initial imperfection in shape. Initial imperfections in the shape of the shell usually arise during the manufacture, transportation and installation of products, as well as during the design of the shell elements.

It is known that the initial imperfections of the shape play a significant role in the behavior of thin-walled shells; therefore, it is very important to take them into account when calculating shells for strength and stability. Often these imperfections are accounted for as initial deflection deviations. In the problem under consideration, we take the initial deflection of the deflection in the same form as the total deflection, that is,

$$w_o = f_o(sin\frac{m\pi x}{L}sin\frac{ny}{R} + \psi\, sin^2\frac{m\pi x}{L} + \varphi) \quad (2)$$

For this problem, the initial equations will be

$$\left.\begin{aligned} &\nabla^4(w-w_o) = \frac{12}{h^3}[L(w,F) + \nabla_k F + \tilde{E} + \tilde{P}] \\ &\nabla_\beta^4 F = -B_{11}\left[\frac{1}{2}\big(L(w,w) - L(w_o,w_o)\big) + \nabla_k w - \nabla_k w_o\right] + \\ &B_{11}\int_o^t G(t-\tau)\left[\frac{1}{2}\big(L^*(w,w) - L^*(w_o,w_o)\big) + \nabla_k w - \nabla_k^* w_o\right]d\tau \end{aligned}\right\} \quad (3)$$

Substituting (1) and (2) into the right-hand side of the second equation (3) and integrating, we determine the stress function in the middle surface

$$F = B_{11}\left(K_1 cos\frac{2m\pi}{L} + K_2 cos\frac{2ny}{R} + K_3 sin\frac{m\pi x}{L}sin\frac{ny}{R} + K_4 sin^3\frac{m\pi x}{L}sin\frac{ny}{R} - \frac{Py^2}{2} - \frac{qR}{2h}x^2\right) \quad (4)$$

here q is the intensity of the external pressure;

P is the intensity of dynamic compressive forces applied to the ends of the shell.

Applying the Bubnov-Galerkin method to the first equation of system (3), we obtain

$$\int_o^L \int_o^{2\pi R} X \sin r\, x \sin s\, y dx dy = o, \tag{5}$$

$$\int_o^L \int_o^{2\pi R} X \sin^2 r\, x dx dy = o, \tag{6}$$

where

$$X = \frac{h^2}{12}\nabla^4(w - w_o) - L(w, F) - \nabla_k F + \rho \frac{\partial^2 w}{\partial t^2}, \tag{7}$$

Integrating (5) and (6) with allowance for (1), (4), and (7), we obtain the equation of motion for the shell.

$$\left.\begin{aligned}
&\frac{d^2\xi_1}{d\tau^2} + C_1\left(1 - \frac{P}{T_1}\right)\left[(1+a_1)\xi_1 + a_2\xi_1\xi_2 + a_3\xi_1\xi_2^2 + a_4\xi_2 + a_5\xi_1^2 + a_6\xi_1^3 + a_7 + a_8\xi_1^2\xi_2\right] = \\
&= (\tilde{a}_1 + \tilde{a}_6\xi_2)\times\int_0^\tau G(\tau - s)\xi_1(s)ds + (\tilde{a}_2 + \tilde{a}_{11}\xi_2)\int_0^\tau G(\tau - s)\xi_1\xi_2 ds + (\tilde{a}_7\xi_1 + \tilde{a}_3)\int_0^\tau G(\tau - s)\xi_1^2(s)ds + \\
&+ (\tilde{a}_4 + \tilde{a}_8\xi_1)\int_0^\tau G(\tau - s)\xi_2 ds + (\tilde{a}_5 + \tilde{a}_9\xi_1 + \tilde{a}_{10}\xi_2)\int_0^\tau G(\tau - s)ds + \tilde{a}_{12}\xi_1\int_0^\tau G(\tau - s)\xi_1 ds + C_1\frac{P}{T_1}\xi_{1,0} = 0 \\
&\frac{d^2\xi_2}{d\tau^2} + C_2\left(1 - \frac{P}{T_2}\right)\left[\xi_2 + b_1\xi_1^2\xi_2 + b_2\xi_1^2 + b_3\xi_1 + b_4\times\xi_1\xi_2 + b_5\right] - C_2\frac{P}{T_2}\xi_{2,0} = \tilde{b}_1\int_0^\tau G(\tau - s)\xi_2 ds + \\
&+ (\tilde{b}_2\xi_2 + \tilde{b}_3)\int_0^\tau G(\tau - s)\xi_1 ds + \tilde{b}_4\int_0^\tau G(\tau - s)\xi_1^2 ds + (\tilde{b}_6 + \tilde{b}_5\xi_1)\int_0^\tau G(\tau - s)\xi_1\xi_2 ds
\end{aligned}\right\} \tag{8}$$

the following dimensionless parameters are introduced here:

$$\xi = \frac{f}{h}, \xi_0 = \frac{f_0}{h}, \hat{P} = \frac{P}{B_{11}}\frac{R}{h},$$

$$\mathrm{T}_1 = B_{11}k_1\hat{\mathrm{P}}_0, T_0 = \frac{1}{(m\pi)^2 k_1\left(1 - \frac{\mathrm{P}}{T_1}\right)},$$

$$\mathrm{T}_1 = B_{11}\left(\frac{1}{4\beta_3(m\pi k_2)^2} - \frac{(m\pi k_3)^2}{6}\right)$$

When solving systems of equations (8) and in other dynamic problems of viscoelasticity, we usually encounter some difficulties, one of which is the calculation of the integral operators

$$\int_0^t G(t-\tau)\xi_1(\tau)d\tau, \int_0^t G(t-\tau)\xi_1^2(\tau)d\tau, \int_0^t G(t-\tau)\xi_1\xi_2(\tau)d\tau, \tag{9}$$

included in the equations of motion (8).

3. METHODOLOGY.

Before proceeding to the solution of system (8), it is necessary to calculate convolutions of the form (9). In the system of equations (8), the argument t does not take part in an explicit form. When $t = 0$ the following conditions are met:

$$\xi_1(0) = \xi_1^0, \xi_2(0) = \xi_2^0, \dot{\xi}_{it} = \tilde{\xi}_1^0, \dot{\xi}_{2t} = \tilde{\xi}_2^0.$$

because there are always solutions in homogeneous differential equations that differ from zero only under the conditions $t = 0$

$$\left.\begin{matrix} y_i(o) = y_i^0(o) \\ \dot{y}_{it}(o) = 0 \end{matrix}\right\}, \left.\begin{matrix} y_i(o) = 0 \\ \dot{y}_{it}(o) = 0 \end{matrix}\right\}, \left.\begin{matrix} y_i(o) = y_i^0 \\ \dot{y}_{it}(o) = \tilde{y}_i^o \end{matrix}\right\}$$

For carefully manufactured casings, the amplitude of the initial deflection can be calculated to be approximately 0.001; 0.0001 times the thickness. These data, as shown in [1], are in satisfactory agreement with the results of experiments related to carefully manufactured samples. Therefore, we will accept

$$\xi_1^o = \xi_2^o = 0.1\cdot 10^{-3}, \tilde{\xi}_1^0 = \tilde{\xi}_2^o = 0, \tag{10}$$

The $\xi_1(\tau)$, $\xi_2(\tau)$ functions included in the integral operators in (8) can be represented as a power series [4]

$$\xi_1(\tau) = \sum_{K=0}^{n} P\,\tau^K, \xi_2(\tau) = \sum_{K=0}^{n} q_K\,\tau^K, \quad (11)$$

Let $\xi_1(\tau), \xi_2(\tau)$ be a real smooth function with the integral $0 \le \tau \le \infty$, n - the derivative with respect to τ. Then the functions ξ_1, ξ_2 can be expanded in a Taylor series at the point $\tau_0 = 0$.

$$\left.\begin{aligned} \xi_1(\tau) = \xi_1(0) + \xi_1^1(0)\tau + \tfrac{1}{2!}\xi_1''(0)\tau^2 + \ldots + \tfrac{1}{n!}\xi_1^{(n)}(0)\tau^n \\ \xi_2(\tau) = \xi_2(0) + \xi_2^1(0)\tau + \tfrac{1}{2!}\xi_2''(0)\tau^2 + \ldots + \tfrac{1}{n!}\xi_2^{(n)}(0)\tau^n \end{aligned}\right\} \quad (11)$$

Comparing the series (11) we find the unknown coefficients P_K, q_K

$$\left.\begin{aligned} P_0 &= \xi_1(0) \\ P_1 &= \xi_1'(0) \\ P_2 &= \tfrac{1}{2!}\xi_1''(0) \\ &\ldots \\ &\ldots \\ P_n &= \tfrac{1}{n!}\xi_1^{(n)}(0) \end{aligned}\right\} \quad (12) \qquad \left.\begin{aligned} q_0 &= \xi_2(0) \\ q_1 &= \xi_2'(0) \\ q_2 &= \tfrac{1}{2!}\xi_2''(0) \\ &\ldots \\ &\ldots \\ q_n &= \tfrac{1}{n!}\xi_2^{(n)}(0) \end{aligned}\right\} \quad (13)$$

The derivatives $\xi_1^n(0), \xi_2^n(0)$ $(n = 1,\ 2,\ 3)$ are determined from the system of equations (8) with $\tau = 0$, then (11) Taking into account (12-13) will take the following form

$$\left.\begin{aligned} \xi_1(\tau) = \sum_{k=0}^{n} \tfrac{1}{K!}\xi_1^{(k)}(0)\tau^k \\ \xi_2(\tau) = \sum_{k=0}^{n} \tfrac{1}{K!}\xi_2^{(k)}(0)\tau^k \end{aligned}\right\} \quad (14)$$

According to d'Alembert's signs, if $\lim_{n\to\infty} D_n^* = D^*$ exists, then with $D^* \prec 1$ this series is called absolutely convergent, with $D^* \succ 1$ - absolutely divergent, where

$$D_n^* = \frac{|a_{n+1}t^{n+1}|}{|a_n t^n|},$$

In the case under consideration

$$D_n^* = \frac{1}{k+1}, \bar{R} = |\tau_0| \lhd \frac{1}{\lim_{k\to\infty}\frac{1}{k+1}} \to \infty, \quad (15)$$

where $\overline{R}$ is the radius of convergence. This means that the series (14) under consideration absolutely converge in the $-\infty \prec \tau_0 \prec \infty$ interval and in these series, it is possible to limit ourselves to four terms, since the other terms rapidly tend to zero.

Substituting (14) in $\int_0^\tau G_{11}(\tau - S)\xi_1(S)dS$ and making the substitution $\tau - S = u$, we get

$$\int_0^\tau e^{-\beta(\tau-s)}(\tau - s)^{\alpha-1}\xi_1(s)ds = \int_0^\tau \frac{e^{-\beta(\tau-s)}}{(\tau - s)^{1-\alpha}}\sum_{k=0}^{n} P_k s^k\,ds = \int_0^\tau \frac{e^{-\beta u}}{u^{1-\alpha}}\sum_{k=0}^{n} P_k(\tau_k - u)^k\,du$$

$$= \sum_{k=1}^{n} P_{1,n-k}(\tau)\int_0^\tau \frac{e^{-\beta u}}{u^{1-\alpha}}u^k du - \sum_{k=0}^{n} P_k\tau^k \int_0^\tau \frac{e^{-\beta u}}{u^{1-\alpha}}du, \quad (16)$$

where

$$P_{1,n-k} = \sum_{k=0}^{n-k} b_i\tau^i,$$

Integral $I = \int_0^\tau l^{-\beta u}u^{-\alpha-1}du$is a tabulated function. Values in the form of a table are given in [4] or integration can be performed numerically, as after integration by parts once, the singularity of the function disappears. Integrating $I_2 = \int_0^\tau l^{-\beta S}S^{\alpha+K-1}$ by

$$\int_0^\tau e^{-\beta s}\,s^{\alpha+k-1}ds = P_{2,k}(\tau)e^{-\beta\tau}\tau^{\alpha-1} + \gamma_k\int_0^\tau e^{-\beta s}s^{\alpha-1}ds, \quad (17)$$

where

$$P_{2,k}(\tau) = \sum_{j=0}^{k} c_j\,\tau^j, P_{2,k} = 0, \gamma_k = \prod_{j=1}^{k}\frac{k - j + \alpha}{\beta}, \gamma_0 = 1.$$

Substituting (17) into (16), we define the expression for the integral convolutions

$$\int_0^\tau \frac{e^{-\beta(\tau-s)}}{(\tau-s)^{1-\alpha}} \sum_{k=0}^n P_k s^k ds = \sum_{k=1}^n P_{1,n-1}\left[P_{2,k}\frac{e^{-\beta\tau}}{\tau^{1-\alpha}} + \gamma_k \int_0^\tau \frac{e^{-\beta}}{s^{1-\alpha}} ds\right] - \sum_{k=0}^n P_k \tau^k \int_0^\tau \frac{e^{-\beta s}}{s^{1-\alpha}} ds, \quad (18)$$

Similarly converted and integral operators

$$\int_0^\tau G(\tau-s)\xi_2(s)ds, \int_0^\tau G(\tau-s)\xi_1(s)\xi_2(s)ds, \int_0^\tau G(\tau-s)\xi_1^2(s)ds, \quad (19)$$

Further, the system of equations (8), taking into account (19), is solved by the numerical Runge-Kutta method with the following initial data

$$\frac{\beta_{11}}{\rho_0 c^2} = 1, \frac{\beta_{22}}{\beta_{11}} = n_1 = 0{,}78; \frac{\beta_{22}}{\beta_{11}} = n_2 = 0{,}004; \frac{2\beta}{\beta_{11}} = n_3 = 0{,}6;$$

$$\beta_1 = \frac{n_1}{n_1 - n_2^2}, k_1 = 0.01; k_2 = 0.01; G_{11}(t) = A_o e^{-\alpha_o t} t^{\beta_0 - 1},$$

$$A_o = 0.0048; \alpha_o = 0.2; \beta_o = 0.05; \frac{G_{12}}{G_{11}} = N_3 = 0.06; \frac{G_{22}}{G_{11}} = N_2 = 0.38;$$

$$\frac{G}{G_{11}} = 0.107; P = st, t^* = \tau = \frac{ct}{R}$$

4. ANALYSIS AND RESULTS.

For visco-elastic shells, the nature of the change in the deflections ξ_1, ξ_2 in time at various dynamic loads, given in Figures 2-4. Various series of curves at $n = 3$ in Fig. 2a refer to those loaded with $S = 0{,}8;\ 1{,}2;\ 2 \cdot 10^5 \frac{MPa}{s}$ velocities for viscoelastic shells. In this case, significant increases in the ξ_1 and ξ_2 deflections are observed in the $t^* = 20 \div 40$ time interval at $S = 3 \cdot 10^5 \frac{MPa}{s}$. The influence of the number of waves n at a constant loading rate S on the changes in the deflections ξ_1, ξ_2 for a viscoelastic shell is shown in Fig. 3 a.

From curves 1-8 (Fig. 3a) it can be seen that the early increases in the deflections ξ_1, ξ_2 are observed with the number of waves $n = 7$. In addition, the deflections for all n waves increase in the $t^* = 20 \div 40$ time interval. The change in the deflections ξ_1, ξ_2 in time at the loading rate of the $S = 5 \cdot 10^5 \frac{MPa}{s}$ and the numbers of waves $n = 5,\ 9$ is shown in Fig.4a. Here, an increase in deflections was noted with the number of $n = 5$ waves at the time $t^* = 12 \div 20$. The change in ξ_1, ξ_2 is influenced by the loading rate $S \succ 1 \cdot 10^5 \frac{MPa}{s}$ and the number of n waves (Fig. 3b). The more S, the faster the increase in the absolute values of the deflections. The dynamic critical load is approximately 4 times the upper static critical load, i.e. with an increase in the loading rate, P_{cr}^d increases. The influence of the viscosity of the shell material on the nature of the change in the deflections ξ_1, ξ_2 is shown in Fig. 4b.

With an increase in the viscosity of the material, the values of the deflections ξ_1, ξ_2 at a constant loading rate ($S = 2 \cdot 10^5 \frac{MPa}{s}$) (Fig. 4b) increase. Figure 2.b shows the curves $\xi_1(t^*)$, $\xi_2(t^*)$ for an isotropic and orthotropic shell at a loading rate of $S = 2 \cdot 10^5 \frac{MPa}{s}$ and the number of $n = 5$ waves. The parameters of the considered isotropic and orthotropic shell are taken to be the same, except for their rigidity. The stiffness ratios for the annular and axial directions for the isotropic shell are equal to $B_{22}/B_{11} = 1$, and for the orthotropic $\frac{B_{22}}{B_{11}} = 0.78$. Curves 1, 2 and 5, 6, respectively, reflect the dependence of $\xi_1 \sim t^*$, $\xi_2 \sim t^*$ for an isotropic elastic and viscoelastic shell, and curves 3, 4 - for a viscoelastic orthotropic shell. It can be seen that with an increase in the rigidity of B_{11}, the rate of increase in the deflections ξ_1, ξ_2 and the maximum from the value decrease. Taking into account the viscosity of the material of the isotropic shell, as well as the orthotropic deflections, increase, and the nature of the motion becomes more complicated.

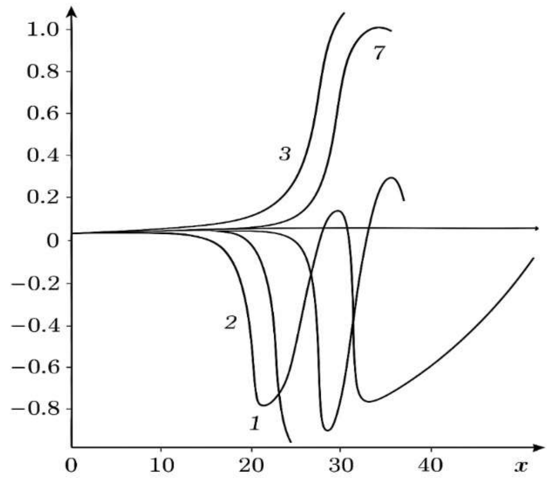

Figure. 2a. The relationship between ξ_1, ξ_2 and $\hat{t}$ at various S and N.

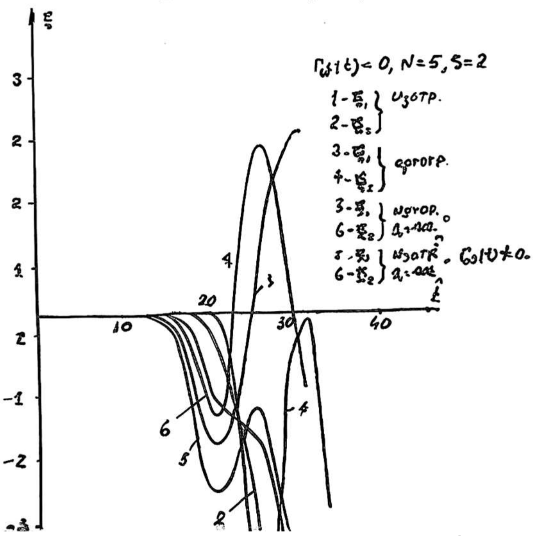

Figure. 2b. The relationship between ξ_1, ξ_2 and $\hat{t}$ at various S and N.

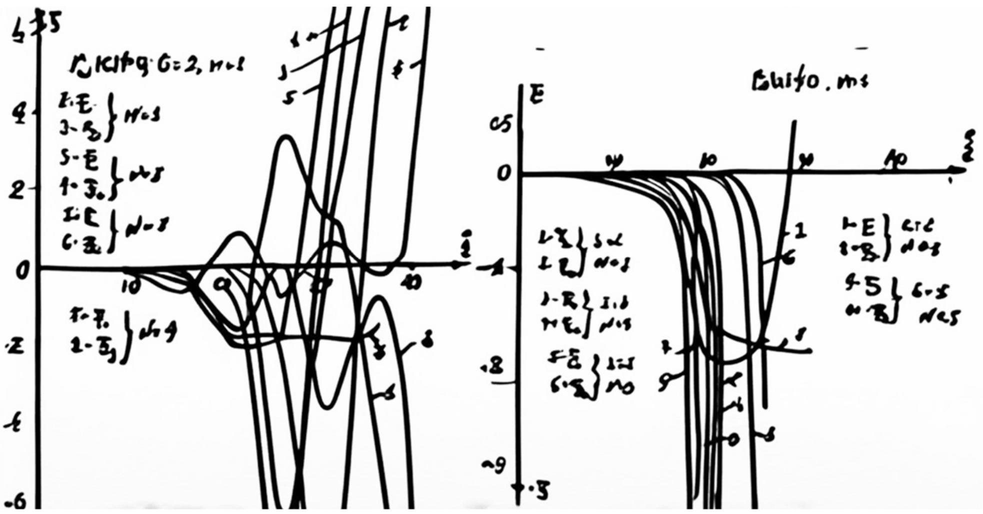

Figure. 3. Dependence between ξ_1, ξ_2 and $\hat{t}$ at different numbers of waves N(a) and loading rate S(b).

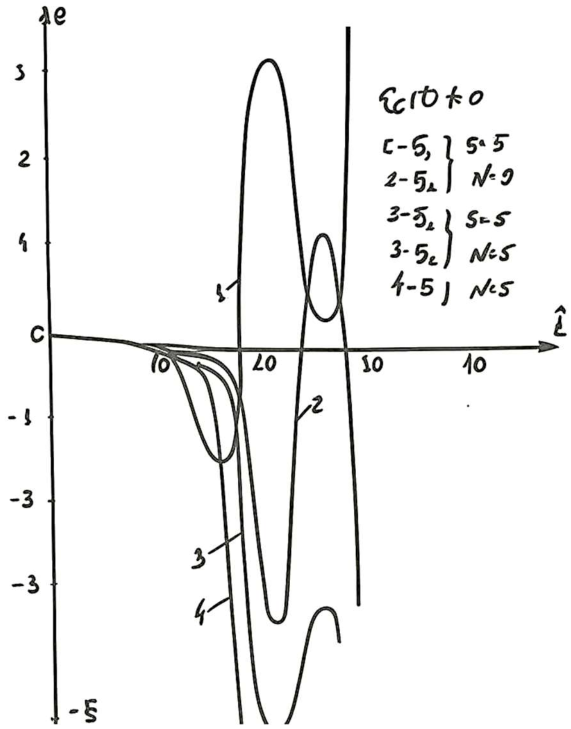

Figure.4a. Change in the deflection ξ_1, ξ_2 depending on the number of *N* waves.

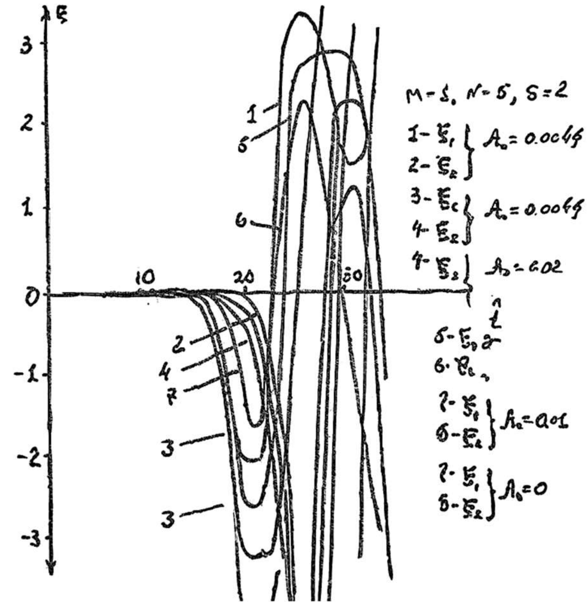

Figure. 4b. Change in deflection ξ_1, ξ_2 depending on the viscous properties of the material.

5. CONCLUSIONS.

In this work, the problem of nonlinear dynamic stability of orthotropic cylindrical shells with viscoelastic properties subjected to compressive loads has been investigated within a geometrically nonlinear formulation. On the basis of the Boltzmann–Volterra hereditary theory, constitutive relations describing the time-dependent behavior of the shell material were incorporated into the governing equations. The application of the Bubnov–Galerkin method allowed the original partial integro-differential equations to be transformed into a system of nonlinear ordinary differential equations, which were solved numerically using the Runge–Kutta method.

The obtained results demonstrate that the dynamic response of viscoelastic cylindrical shells is strongly influenced by the loading rate, material viscosity, and the number of circumferential and longitudinal waves. It has been established that an increase in the loading rate leads to a significant growth of the dynamic critical load in comparison with the static critical load. For the considered cases, the dynamic critical load may exceed the static one by approximately four times, which confirms the necessity of dynamic analysis when assessing shell stability.

It is also shown that an increase in material viscosity accelerates the growth of deflections and promotes earlier onset of dynamic buckling. Furthermore, the presence of initial geometric imperfections considerably reduces the stability margin and intensifies the transition from stable vibrations to unstable motion. Orthotropic shells exhibit different stability characteristics compared with isotropic ones, and the stiffness ratio in axial and circumferential directions plays an important role in determining the buckling behavior.

The results obtained in this study can be used in the design and analysis of thin-walled shell structures operating under dynamic compressive loads. The developed approach provides a reliable theoretical basis for predicting dynamic buckling and may be extended to other types of shells and loading conditions.

REFERENCES

[1] Author(s), M.H. Ilyasov, Dynamic stability of viscoelastic plates, Int. J. Eng. Sci. 45 (2007) 111–122.
[2] R.T.A. Robinson, S. Adali, Nonconservative stability of viscoelastic rectangular plates with free edges under uniformly distributed follower force, Int. J. Mech. Sci. 107 (2016) 150–159.
[3] Author(s), A. Ilyushin, B. Pobedrya, Fundamentals of Mathematical Theory of Thermoviscoelasticity, Nauka, Moscow, 1970.
[4] A.S. Vol'mir, Nonlinear Dynamics of Plates and Shells, Nauka, Moscow, 1972.
[5] A.S. Vol'mir, Shells in Fluid and Gas Flow: Problems of Hydroelasticity, Nauka, Moscow, 1979.
[6] E. Grigolyuk, V. Mamai, Non-Linear Strain of Thin-Walled Constructions, Nauka, Moscow, 1997.
[7] M.A. Koltunov, On the calculation of flexible gently sloping orthotropic shells with linear heredity, Bull. Moscow State Univ. 5 (1964) 79–88.
[8] Nonlinear flutter response of pre-heated functionally graded panels, Int. J. Comput. Mater. Sci. Eng. 7 (1&2) (2018) 1850012. [75] F.W. Xia, Y.P. Feng, D.W. Zhao, Finite element multi-mode approach to thermal postbuckling of functionally graded p
[9] A.I. Karimov, S.Sh. Baxritdinov, M.G. Azambayev. Theoretical Study of the Movement Process in the Vibration of Cotton Seeds. Journal of Advanced Research in Dynamical and Control Systems. Vol. 12, 05-Special Issue, pp.835-840 (2020). http://doi.org/10.5373/JARDCS/V12SP5/20201823
[10] R. Muradov, B. Mardonov, A.I. Karimov. Theoretical and Experimental Studies of the Effect of Inclined Scraper on Raw Cotton from Mech Surface. World Journal of Mechanics, USA. 2014, 4, 371-377.
[11] S.Khusanov,A.Makhkamov,R.Muradov,A.I.Karimov. Study of the Effect of the Mobile Floor of the Separator Devise on the Cotton Section. International Jurnal of Psychosocial Rehabilitation,Vol.24, Issue 05,2020.ISSN:1475-7192.6473-6481 pp.
[12] M. Ismanov, A. Karimov. The action of shock waves on cylindrical panels. AIP Conference Proceedings, Vol.3045, Iss.1, Article ID 030101 (2024). https://doi.org/10.1063/5.0197285
[13] Ismanov M., Azizbek A., Hushnid M, Dedaxuja F. Theoretical and experimental study of the law of distribution of non-stationary heat flux in raw cotton stored in the bunt. AIP Conference Proceedings, Vol.2789, Iss.1, Article ID 040106(2023). https://doi.org/10.1063/5.0145484
[14] A. Anvarjanov, S. Kozokov, R. Muradov. Analysis of research on changing the surface of the grid in a device for cleaning cotton from fine impurities. Scientific and Technical Journal Namangan Institute of Engineering and Technology. Vol. 9, Iss.1 (2024).
[15] D. Qodirov, M. Ismanov. Stable algorithms for the identification of delayed control objects based on input and output signals. AIP Conference Proceedings, Vol.3045, Iss.1, Article ID

030103 (2024). https://doi.org/10.1063/5.0197284

[16] A. Karimov, M. Ismanov, S. Bahriddinov. Theoretical study of the law of distribution of non-stationary heat flux in vertical and horizontal layers of raw cotton (stored in a cotton riot). AIP Conference Proceedings, Vol.3122, Iss.1, Article ID 100005 (2024). https://doi.org/10.1063/5.0217431

[17] N. Sharibaev, A. Jabborov, R. Rakhimov, Sh. Korabayev and R. Sapayev. A new method for digital processing cardio signals using the wavelet function. BIO Web of Conferences. 2024. Vol. 130, Article No 04008. https://doi.org/10.1051/bioconf/202413004008

[18] Sh. Korabayev, J. Soloxiddinov, N. Odilkhonova, R. Rakhimov, A. Jabborov and A.A. Qosimov. A study of cotton fiber movement in pneumomechanical spinning machine adapter. E3S Web of Conferences. 2024. Vol. 538, Article No 04009. https://doi.org/10.1051/e3sconf/202453804009